ISBN: 978-3-95450-214-1 ISSN: 2673-5490 doi:10.18429/JACoW-IPAC2021-THPAB239

IMPEDANCE OPTIMIZATION OF THE EIC INTERACTION REGION VACUUM CHAMBER *

A. Blednykh †, E. C. Aschenauer, M. Blaskiewicz, C. Hetzel, M. Sangroula, G. Wang, H. Witte
Brookhaven National Laboratory, Upton, NY, USA

Abstract

The interaction region chamber has a complex geometry at the crossing location of electron and proton beam pipes. In the direction of the electron beam, the pipe is designed in a way to avoid joints with cavity characteristics. The horizontal slot on the upstream side and the tapered transition on the downstream side are applied to minimize the IR-chamber contribution to the total impedance of the electron ring and to avoid generating Higher Order Modes and heating-related issues. The synchrotron radiation mask is included to protect the IR chamber from synchrotron radiation without significant aperture reduction. In the direction of the proton beam, the main area for optimization is the transition area right after the detector.

INTRODUCTION

The interaction region (IR) vacuum chamber design for the electron-ion collider (EIC) project has been iterated on several times since the EIC CDR [1]. Aggressive parameters of the electron beam with high average current $I_{av} = 2.5$ A within $M = 1160$ bunches and a $\sigma_s = 7$ mm bunch length motivates the IR chamber design to achieve stable operation without generating Higher Order Modes (HOMs) and with a possibility to mitigate beam-induced heating. One of the major contributions to the local impedance are discontinuities where the electron and hadron beam pipes merge. The electron pipe geometry needs to be designed so it does not block the propagation of forward moving particles resulting from collisions within a 25 mrad cone starting from the interaction point. This requirement complicates the transition between the two beam pipes. As a first attempt, the electron beam pipe was grounded to the hadron pipe with a small taper angle. Half of the taper was left open. This arrangement resulted in a cavity type structure between the area of the electron pipe grounding and the larger hadron beam pipe. To reduce the cavity effect, the electron beam pipe was extended, and a horizontal slot was added on one side to provide clearance for the particle propagation to the forward detector (Fig. 1). As it is well-known the impedance of a slot, as a single element, provides the smallest contribution to the total impedance of the storage ring compared to the geometry of two merging beam pipes, tapered transition or a cavity type structure. As it is shown in Fig. 1, the electron beam propagates through the circular vacuum chamber with a 60 mm diameter and sees the oval horizontal slot on the upstream (US) side of the IR chamber with an opening large enough for the forward moving hadron collision particles to pass cleanly. The downstream (DS) side of the chamber has a

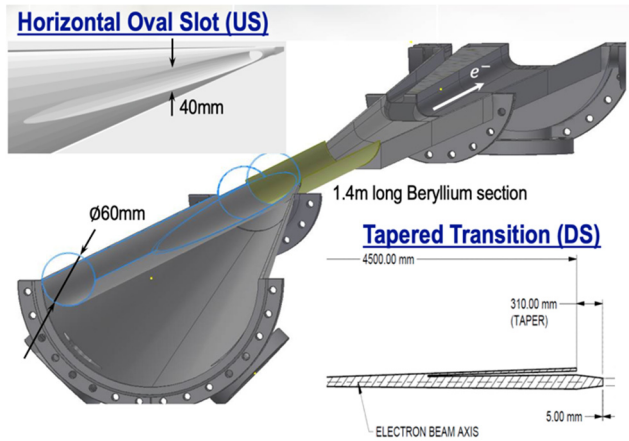

Figure 1: One-half of the IR chamber.

tapered transition from a flat rectangular chamber to a standard circular shape of the EIC vacuum chamber. The main idea is to keep the vertical full aperture fixed (60 mm) and change the beam pipe horizontally to accommodate the synchrotron radiation (SR) fan.

In Figs. 2, 3, 4 and 5 we plot the real part of the longitudinal impedance and the loss factor as a function of bunch length for US and DS of the IR chamber, assuming a diameter of the middle long Beryllium section is the same as the diameter of the standard vacuum chamber, 60 mm. Two sides of the vacuum chamber are far enough apart that each side can be calculated separately. The total length of the IR chamber is 9 m long and it requires significant essential computer resources to complete the simulations. To protect the IR chamber from synchrotron radiation the final photon absorber (FPA) is planned to be installed in the electron vacuum chamber as it is shown in Fig. 6 (tapered collimator). The real part of the longitudinal impedance without the FPA looks HOM's free in the frequency range up to 14 GHz. The estimated loss factor for a 7 mm bunch length is $k_{loss} = 1.3$ mV/pC. Hence the power loss is $P_{loss} = T_0 I_{av}^2 k_{loss}/M = 90$ W at average current $I_{av} = 2.5$ A within $M = 1160$ bunches, where $T_0 = 12.79$ μs is the revolution period. A water-cooling system is under consideration.

Installation of the SR final photon absorber (Fig. 6) on the US of the electron vacuum chamber shrinks the aperture and leads to generation of the high-frequency impedance and hence increases the loss factor up to $k_{loss} = 4.5$ mV/pC (Fig. 3, green trace).

The impedance and the loss factor of the DS side of the IR chamber (Figs. 4 and 5) look predictable because of the smooth transition from a rectangular to the circular

* Work supported by Brookhaven Science Associates, LLC under Contract No. DE-SC0012704 with the U.S. Department of Energy.
† blednykh@bnl.gov

ISBN: 978-3-95450-214-1 ISSN: 2673-5490 doi:10.18429/JACoW-IPAC2021-THPAB239

chamber profile. The geometric dimensions of the IR chamber will be a subject of discussion until the design is finalized.

Since the IR chamber is a complex geometry, we continuously cross-checking the numerical data using different codes: ECHO 3D [2], GdfidL [3], CST [4] and the code developed by Sasha Novokhatski. Here we discuss comparison of the GdfidL and the ECHO 3D codes for the US and DS sides of the IR chamber. Since the ECHO 3D code is a singular processor code, the computer resources needed are on a level of the workstation or the personal laptop, while the GdfidL code is a Linux-based software and is installed on the new powerful institutional cluster at BNL. To perform the numerical simulations, we increased the reference bunch length up to 12 mm. The results of the longitudinal wakefields $W(s)$ comparing US and DS are presented in Figs. 7 and 8. The GdfidL code computes the geometries (4.5 m long) with a 250 μm step size. To check that the results agree, a 200 μm step size has been applied for the US side of the IR chamber, where the thickness of the electron beam pipe is 1 mm. Figure 7 shows two traces (gray and blue) that almost perfectly overlap. The ECHO 3D wakefield $W(s)$ (dashed red trace) simulated for a 400 μm agrees with GdfidL $W(s)$ for the DS side and is slightly different for the US side of the IR chamber. Figure 9 shows the results of the FPA optimization for a 10 mm and 350 mm gap. The low-frequency results are very similar, there are significant differences as the frequency increases. It should be noted here that the loss factor does not change on the FPA gap in considered range.

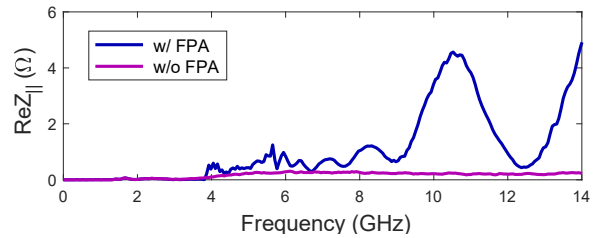

Figure 2: The real part of the longitudinal impedance for the **US** of the IR chamber with and without FPA.

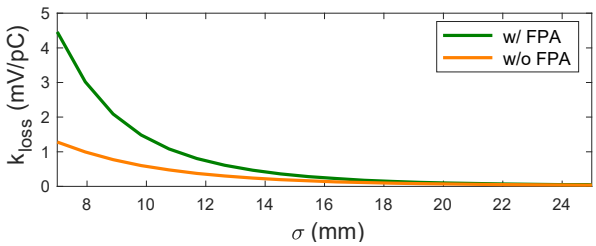

Figure 3: The loss factor as a function of bunch length for the **US** of the IR chamber with and without FPA.

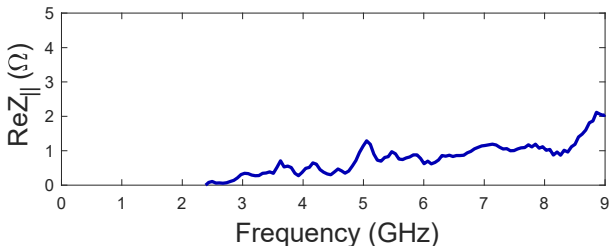

Figure 4: The real part of the longitudinal impedance for the **DS** of the IR chamber.

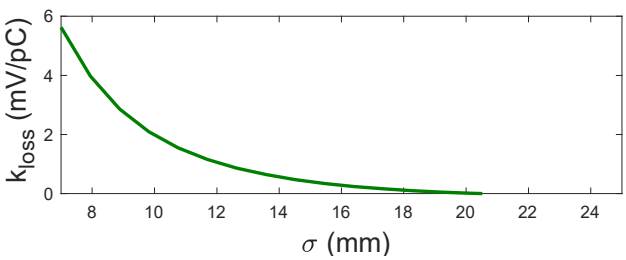

Figure 5: The loss factor as a function of bunch length for the **DS** of the IR chamber.

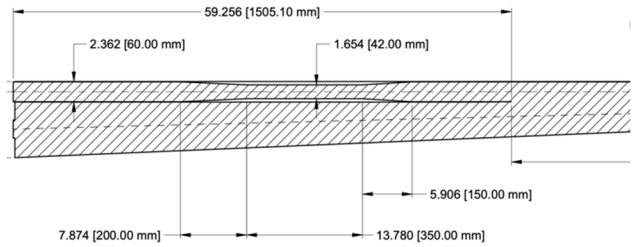

Figure 6: The US of the IR chamber with FPA installed.

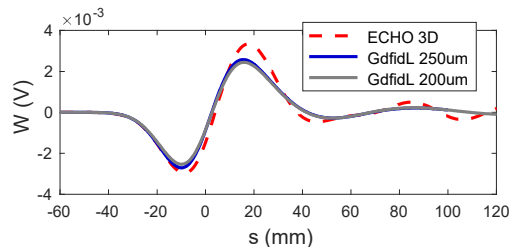

Figure 7: The longitudinal short-range wakefield simulated for the **US** of the IR chamber with a 12 mm bunch length for comparison of two codes.

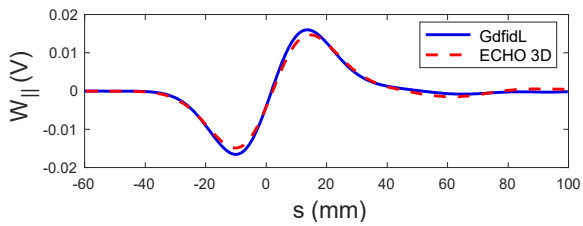

Figure 8: The longitudinal short-range wakefield simulated for the **DS** of the IR chamber with a 12 mm bunch length for comparison of two codes.

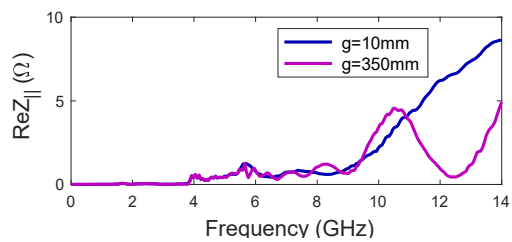

Figure 9: Real part of the longitudinal impedance for FPA with g = 10 mm and 350 mm.

ISBN: 978-3-95450-214-1 ISSN: 2673-5490 doi:10.18429/JACoW-IPAC2021-THPAB239

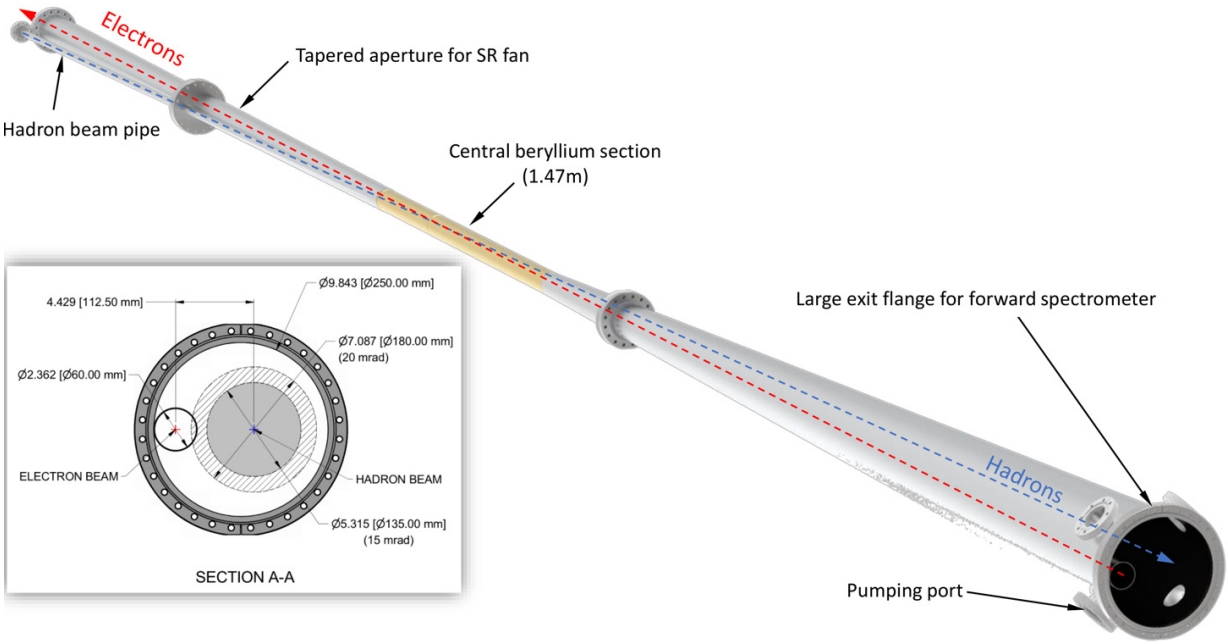

Figure 10: Design of the IR chamber for the EIC project.

In Fig. 10, we present the preliminary design of the IR chamber. The IR interface requirements present several complex challenges which require close attention to detail. The vacuum chamber in this region becomes the primary interface between the particle beams and the experiment detector components.

One of the first challenges is to meet all of the geometrical requirements of the interaction point vicinity of the IR. First and foremost the vacuum chamber is designed to allow clear passage of the two high energy particle beams. Space constraints for the SR fan resulting from the strong focusing electron quadrupoles is taken into account. Designing the central vacuum pipe with a large diameter would easily meet these requirements and would also provide large conductance to the vacuum pumps that is required to achieve the lowest possible pressure in the detector region. However, to ensure large acceptance for all the collisions products, the experiment detectors must be placed as close as possible to the interaction point [5]. Since these collision product particles must pass through the walls of the beam pipe, every effort must be made to minimize the vacuum chamber wall thickness near the IP.

It is very important to minimize the dynamic pressure inside the IR vacuum chamber in order to minimize beam-gas interactions. Any synchrotron radiation (direct or scattered) impinging on surfaces will result in a high dynamic pressure from photon induced desorption and surface heating. The particles in the circulating beams can scatter on the residual gas molecules, which can result in high detector backgrounds.

CONCLUSION

The IR vacuum chamber design for the EIC project is in progress. We have confidence that it can be mechanically designed to satisfy all of the required parameters. The next step is optimization of the IR chamber from proton-beam point of view, whose 60 mm bunch length is significantly longer than the 7 mm electron bunch length. The main focus will be on the detector area, where the large exit flange for forward spectrometer will be attached to the standard circular vacuum chamber.

Another most challenging task is to simulate the longitudinal wakefield for a 0.3 mm bunch length (pseudo-Green's function), since we need to include the IR wakefield into the EIC impedance budget [6]. The IR chamber is 9 m long and a moving window algorithm needs to be considered to complete the simulations [7]. However, the accuracy of numerical simulations, for example in GdfidL, dependence on the geometry.

REFERENCES

[1] EIC Conceptual Design Report 2021, https://www.bnl.gov/ec/files/EIC_CDR_Final.pdf

[2] W. Bruns, http://www.gdfidl.de

[3] CST Particle Studio, http://www.cst.com

[4] I. Zagorodnov, "Indirect methods for wake potential integration", *Physical Review Special Topics - Accelerators and Beams*, vol. 9, no. 10, p. 102002, Oct. 2006. doi:10.1103/physrevstab.9.102002

ISBN: 978-3-95450-214-1 ISSN: 2673-5490 doi:10.18429/JACoW-IPAC2021-THPAB239

[5] H. Witte *et al.*, "The Interaction Region of the Electron-Ion Collider EIC", presented at the 12th Int. Particle Accelerator Conf. (IPAC'21), Campinas, Brazil, May 2021, paper WEPAB002, this conference.

[6] A. Blednykh *et al.*, "Impedance Optimization of the EIC Interaction Region Vacuum Chamber", presented at the 12th Int. Particle Accelerator Conf. (IPAC'21), Campinas, Brazil, May 2021, paper THPAB239, this conference.

[7] Lie-Quan Lee, Arno Candel, Cho Ng, and Kwok Ko, "A moving window technique in parallel finite element time domain electromagnetic simulation", SLAC, Menlo Park, CA, USA, Rep. SLAC-PUB-14099, 2010.